Molecular beam epitaxial growth and evaluation of intrinsic and extrinsically doped $Hg_{0.8}Cd_{0.2}Te$ on (100) $Cd_{0.96}Zn_{0.04}Te$

L. He,[a] C. R. Becker, R. N. Bicknell-Tassius, S. Scholl, and G. Landwehr
Physikalisches Institut der Universität Würzburg, D-8700 Würzburg, Germany

(Received 3 September 1992; accepted for publication 8 December 1992)

The structural and electrical properties of (100) $Hg_{1-x}Cd_xTe$ epilayers grown by molecular beam epitaxy have been systematically investigated for different Hg/Te flux ratios. The hillock density, electron concentration and the electron mobility depend strongly on the Hg/Te flux ratio. A minimum in the hillock density correlates well with the highest mobilities and the lowest concentrations. As is well known electrical properties are strongly influenced by structural defects. Structural defects such as twins and defects due to nonstoichiometry can be largely reduced by optimizing the Hg/Te flux ratio. It is shown that an optimum Hg/Te flux ratio exists within a narrow range between 270 and 360 at the growth temperature of 180 °C, in contrast with the larger range of the Hg/Te flux ratio over which single crystalline growth could be maintained. The difficulties encountered in the x value determination from normal transmission curves, i.e., from $E_0(x)$, due to the Burstein–Moss shift are discussed. In order to overcome these difficulties, the x values of the $Hg_{1-x}Cd_xTe$ epilayers were also determined from $E_1(x)$. A calibration of $E_1(x)$ resulted in small but significant discrepancies with the literature. Extrinsic As doping using the δ doping technique is demonstrated and a very high atomic sheet density of 1.2×10^{13} cm^{-2} is obtained.

I. INTRODUCTION

Molecular beam epitaxial (MBE) growth of both high quality intrinsic and extrinsically doped narrow gap $Hg_{1-x}Cd_xTe$ with an x value of 0.20–0.22 are currently important issues in long wavelength detector engineering. They are closely correlated and are very complicated for narrow gap semiconductors in particular. Extrinsic doping techniques and an understanding of the doping mechanism can be established only after the growth parameters for intrinsic materials with high structural quality and good electrical properties have been optimized.

Structural twining defects, namely pyramidal hillocks, are a severe problem encountered in the growth of (100) $Hg_{1-x}Cd_xTe$.[1,2] It has been previously reported that the formation of hillocks is closely related to improper growth conditions,[3–5] a Hg overpressure or Hg clusters are believed to play an important role in the hillock formation. Thus the Hg flux employed in the $Hg_{1-x}Cd_xTe$ growth is one of the most important parameters to be optimized. Structural defects are electrically active, they are a major source of noise in long wavelength infrared $Hg_{1-x}Cd_xTe$ photodiodes, and they cause a reduction in breakdown voltage in metal-insulator-semiconductor capacitors.[5] However, no systematically detailed results of how Hg flux affects the structural and electrical properties have been reported, and no information concerning the correlation of the structural and electrical properties is available.

p-type substitutional doping of $Hg_{1-x}Cd_xTe$ with group V elements, suitable for infrared (IR) detectors and IR lasers, is another important topic of concern. However for conventional MBE growth conditions, it has been reported[6] that the group V elements, As and Sb, are incorporated as donors. It was suggested[7] that group V elements may be incorporated interstitially rather than substitutionally due to their size and low surface mobility. On the other hand, Han *et al.*[8] demonstrated that *p*-type As-doping can be produced in a modulated structure employing the photoassisted MBE (PAMBE) technique.[9] In addition, it has been stressed[10] that establishing cation-stabilized conditions is an important prerequisite for As doping techniques. Laser illumination has been shown[11,12] to enhance Te desorption making the surface more cation-stabilized. To establish a doping technique, it is therefore desirable to understand the mechanism of dopant incorporation and then find a way to enhance this incorporation.

In this article, we present results of a systematic investigation of MBE growth conditions, e.g., the effects of Hg flux on pyramidal hillock density and on electrical properties for the (100) orientation. With an understanding of the growth conditions necessary for good quality intrinsic materials, we have been able to achieve *p*-type As doping for the first time by utilizing the δ doping technique.

II. EXPERIMENTAL DETAILS

Epitaxial growth was carried out in a four-chamber RIBER-2300 MBE system which has been modified to enable the growth of Hg-based materials. These modifications involve the use of a stainless steel Hg cell, providing excellent control of the Hg flux, and changes to the rotatable substrate holder. As a result of the latter modification, a thermocouple is in physical contact with the molybdenum substrate holder during rotation, which enables the substrate temperature to be controlled with an accuracy of better than ±2 °C during growth. The temperature of the molybdenum substrate holder was routinely calibrated at

[a]Shanghai Institute of Technical Physics, Chinese Academy of Sciences, Shanghai 200083, People's Republic of China.

 0021-8979/93/073305-08$06.00 © 1993 American Institute of Physics

the melting point of indium. A low temperature Te cell provided good stability and control of the Te flux.

All samples were grown on lattice matched (100) $Cd_{0.96}Zn_{0.04}Te$ substrates from II-VI Inc. which were carefully screened using x-ray rocking curve topography. Substrate preparation included standard cleaning, chemomechanical polishing techniques, and thermal cleaning in vacuum prior to growth.[13] To avoid diffusion of the remaining impurities on the surface into the epilayers and to obtain an atomically smooth and stoichiometric surface, a CdTe buffer layer of about 1500 Å was grown at 300 °C. Because of the relatively thin $Hg_{1-x}Cd_xTe$ epilayers, it was anticipated that the electrical properties might be influenced substantially by electric charges at the interface, which are a result of conduction band bending in the interface region[14,15] due to the large conduction band offset between $Hg_{1-x}Cd_xTe$ and the CdTe buffer layer. To minimize this interface effect, a second buffer consisting of the intermediate gap $Hg_{0.3}Cd_{0.7}Te$ with a thickness of 300 Å was grown on the initial CdTe buffer in order to distribute the total potential drop between the narrow gap $Hg_{1-x}Cd_xTe$ epilayer and the CdTe buffer.

In order to characterize the effects of the Hg/Te pressure (in this article loosely referred to as flux) ratio on the structural and electrical properties of $Hg_{1-x}Cd_xTe$, a series of samples with x values of 0.206 ± 0.005 were grown with Hg/Te flux ratios between 183 and 550. During $Hg_{1-x}Cd_xTe$ growth at 180 °C, the substrate was rotated at 8–12 rpm and the Hg flux, which was held constant to within $\pm 2\%$, was monitored and recorded by means of an ion gauge at the top of growth chamber during the entire growth period. Reflection high energy electron diffraction (RHEED) was used to monitor the surface structure during growth. A Te flux of 6×10^{-7} Torr was employed for all samples. In order to obtain an x value of approximately 0.20 in the narrow gap $Hg_{1-x}Cd_xTe$ epilayer, the CdTe/Te flux ratio was maintained at 0.3 throughout this investigation with two exceptions. 13 of the 15 epilayers which were grown with this CdTe/Te flux ratio had an x value of 0.206 ± 0.005. The other two had an x value of about 0.19. The growth rate was 3.1 Å/s, and the sample thicknesses were between 2 and 6 μm. To accurately determine the thickness of the epilayers, surface contact masks were put on some of the substrates prior to growth.

RHEED observations demonstrated that single crystalline growth of $Hg_{1-x}Cd_xTe$ for the (100) orientation can be maintained over a wide range of the Hg/Te flux ratio. Well defined RHEED patterns with short streaks were exhibited and remained unchanged during the growth for Hg/Te flux ratios higher than 215 and lower than 517. At the lowest and highest Hg/Te flux ratio studied, 183 and 550, the RHEED pattern was indicative of single crystalline growth during the initial stages of growth, and then after about one hour, additional dots appeared in the RHEED, indicating either the onset of polycrystalline growth or the presence of twins.

An arsenic doped (100) $Hg_{1-x}Cd_xTe$ epilayer was also grown at 180 °C. The doping was carried out by means of the atomic sheet technique. The sample structure consisted of doped, wide gap $Hg_{0.3}Cd_{0.7}Te$ and undoped $Hg_{0.77}Cd_{0.23}Te$ layers. The doping procedure involved interrupting the growth of the wide gap $Hg_{0.3}Cd_{0.7}Te$ layer by closing the CdTe shutter, leaving the Hg shutter open, and opening the Cd shutter. The resulting cation stabilized surface structure was maintained, according to the RHEED pattern, while the As shutter was opened for a predetermined time interval. Growth was resumed by first closing the As and Cd shutters and then opening the CdTe shutter.

Transmission and reflection measurements in the wavelength ranges of the middle IR and the visible were carried out with a Fourier transform spectrometer, IFS88, from Bruker. The epilayer thickness was determined from the interference pattern in the reflection spectrum in the middle IR, which was confirmed by a direct and more accurate measurement of the layer with a depth profiler by using a contact mask on several samples. The electrical properties were determined using the standard van der Pauw method for the Hall effect at 0.3 T for temperatures between 300 and 4.6 K. The electrical contacts were placed on the edges of the samples whose dimensions were 5 and 10 mm. These data were analyzed with a one charge carrier model. A standard Hall structure with dimensions of 200 and 300 μm was etched onto 6 samples. Standard Hall effect measurements as well as Shubnikov de Haas (SdH) oscillation experiments were conducted on these 6 samples at 4.2 K. In addition a multicarrier mobility spectrum analysis[16,17] was carried out for the arsenic doped sample between 0 and 7.5 T. Pyramidal hillocks on the surface of every sample were observed with a microscope with a Nomarski filter. The measured hillock density is the average of hillock densities from various surface regions. It should be mentioned that higher hillock density regions normally existed on the edges or corner of the epilayers, whose total area was $< 3\%$ of the surface. These high density regions are substrate related, and were therefore not included in the calculations of hillock densities.

III. RESULTS AND DISCUSSION

A. Optical measurements and *x* value determination

In order to investigate the influence of the Hg/Te flux ratio during growth on the structural and electrical properties of narrow gap $Hg_{1-x}Cd_xTe$, it is obvious that an accurate determination of the x value of all the epilayers grown under different Hg fluxes is an essential prerequisite. Optical transmission spectra in a wavelength region near the energy gap E_g (or E_0) are generally used to estimate the x value,[18] because of the nondestructive nature and simplicity of this method. However, there are several problems when applying this method to epitaxially grown thin n-type samples. One major problem encountered is the influence of the Fermi level position which can cause a shift of the apparent absorption edge to shorter wavelengths, i.e., the Burstein Moss shift. Transmission measurements reflect the energy difference between the Fermi level and the valence band, which can be appreciably larger than the energy gap E_0 in n-type degenerate $Hg_{1-x}Cd_xTe$ due to the

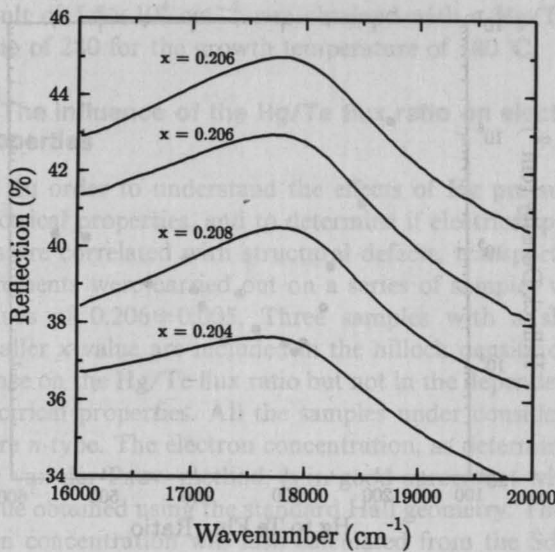

FIG. 1. Examples of room temperature reflection spectra in the visible range. The x values are determined from position of the peaks in the reflection curves.

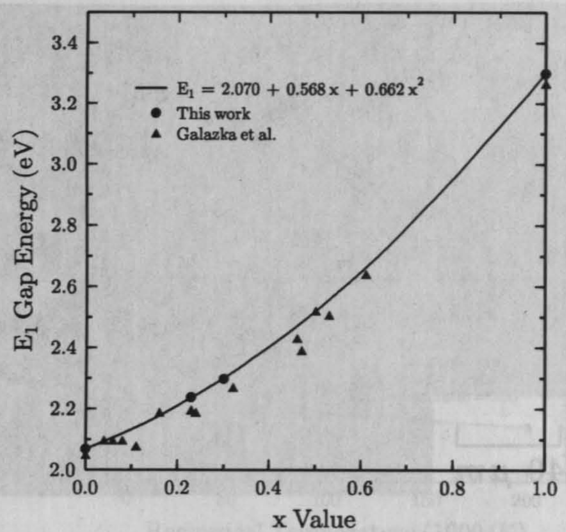

FIG. 2. Calibration curve for the E_1 energy gap versus x value. Both our experimental results and the data from Ref. 24 are presented.

small effective electron mass. In an attempt to estimate the effect of the Burstein Moss shift we calculated the position of the Fermi level as a function of the electron concentration using the Kane model[19] for nonparabolic degenerate bands, and then compared the results with the intrinsic concentrations n_i [20] at different x values.[21] The results demonstrated that an intrinsic $Hg_{1-x}Cd_xTe$ epilayer is degenerate at room temperature if its x value is smaller than 0.19. Furthermore, the results for $x=0.21$ and a carrier concentration of 7×10^{17} cm^{-3} demonstrated that the shift of the apparent absorption edge would correspond to an error of 10% in x. An additional complication in the evaluation of transmission spectra is the presence of interference fringes. Because these epilayers are thin, the absorption edge for these MBE grown samples is much less steep than that for bulk material. Consequently the absorption edge is more strongly influenced by the widely spaced interference fringes, resulting in larger uncertainties in the absorption coefficient α and thus in the x value.

In order to overcome these difficulties in determining the x value from the absorption coefficient in the present study, we have also determined the x value of the $Hg_{1-x}Cd_xTe$ epilayers from the E_1 energy gap ($L6$-$L4,5$)[22] by means of reflection measurements in the visible region. Because the E_1 gap is much larger than the E_0 gap, the effects of degeneracy and interference fringes are essentially eliminated. Examples of room temperature reflection spectra for different x values are shown in Fig. 1. The E_1 energy gap was determined from the peak position of the reflection curve. Because of discrepancies between x values as determined from the E_0 gap and those obtained from the $E_1(x)$ relationship according to the literature,[23–26] we calibrated this relationship again. A MBE grown HgTe layer, a bulk p-type $Hg_{0.702}Cd_{0.298}Te$ sample and a CdTe substrate were employed. The $Hg_{0.702}Cd_{0.298}Te$ sample was provided by the AEG company in Heilbronn, Germany. Its x value was determined using the absorption coefficient method. The resulting calibrated curve are presented in Fig. 2 and are given by

$$E_1(\text{eV})=2.070+0.568x+0.662x^2. \qquad (1)$$

For comparison, values from Galazka and Kisiel[24] are also shown in Fig. 2, which are in fair agreement with our results when one considers the difficulty in determining x for samples grown by different methods. In addition, the crystalline quality of the surface has a large effect on the reflection spectrum. We found that removing about 50 μm from the surface of the mechanically polished CdTe substrate by etching, shifted the peak position 0.195 eV to the higher value shown in Fig. 2.

The x values of the samples studied were determined from the E_0 gap using the standard criterion of $\alpha=1000$ cm^{-1} [27] as well as from the E_1 gap using Eq. (1). The discrepancy between the x values is within experimental uncertainty (±0.002 and ±0.004 for E_1 and E_0, respectively) if the electron concentration is less than 4×10^{17} cm^{-3}. The largest part of this discrepancy in x is caused by uncertainties in α due to the influence of interference fringes. However, this discrepancy increases exponentially for samples with electron concentrations higher than 4×10^{17} cm^{-3}. A discrepancy of about 23% was observed for a sample with an electron concentration of 1.7×10^{18} cm^{-3}.

The optical thickness nd was obtained from the difference in frequency of the interference fringes in reflection spectra in the long wavelength region,[18] i.e., below the E_0 gap. A calibrated value for the refractive index n was determined by measuring the thickness of an epilayer grown on a substrate with a contact mask using a depth profiler. A refractive index $n=3.50$ was obtained for $x=0.208$ at a wavelength of 12 μm, which is in good agreement with the literature.[18]

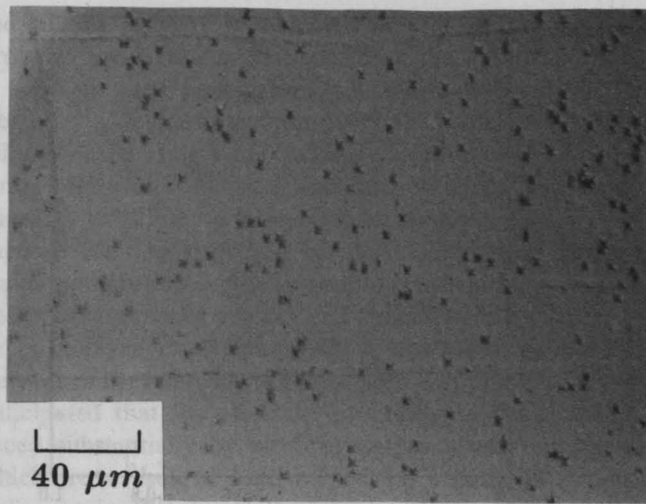

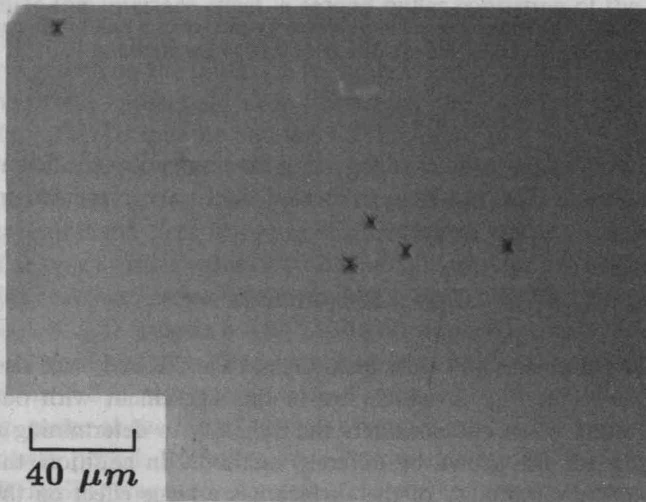

FIG. 3. Photomicrographs showing the surface morphology and the presence of hillocks for (a) an epilayer grown with a Hg/Te flux ratio of 183 and a thickness of 2.0 μm, and (b) an epilayer grown with a Hg/Te flux ratio of 300 and a thickness of 5.8 μm.

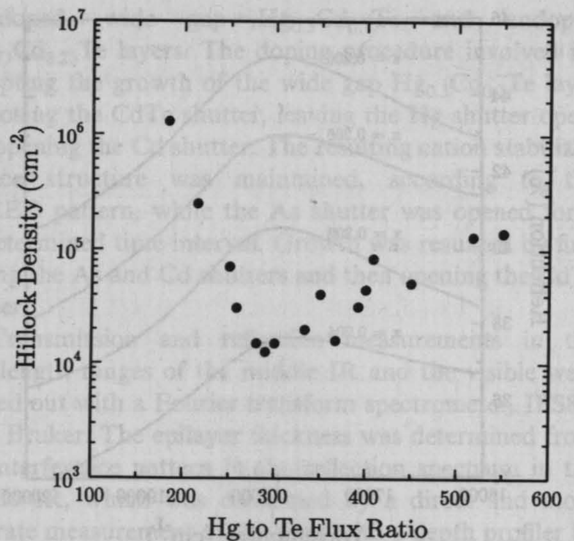

FIG. 4. Hillock density vs Hg/Te flux ratio for all samples.

B. The influence of the Hg/Te flux ratio on structural defects

In order to understand the dependence of hillock formation on the Hg/Te flux ratio and thus to eliminate or reduce the number of hillocks on (100) epilayer surfaces, hillock density measurements were carried out on all samples. Figures 3(a) and 3(b) show examples of two sample surfaces, displaying the presence of hillocks. Figure 3(a) shows a sample grown with a Hg/Te flux ratio of 183 and a thickness of 2.0 μm, and Fig. 3(b) a 5.8-μm-thick sample grown with a ratio of 300. By comparing Figs. 3(a) and 3(b), it can be easily seen that the hillock density depends strongly on Hg pressure, and that the hillock size increases with increasing epilayer thickness. In addition, careful examination revealed that the size was the same for the majority of hillocks on each sample and that high density regions usually occurred near the edges of the epilayer. The dependence of hillock density on the Hg/Te flux ratio is demonstrated in Fig. 4. This dependence is a V-shaped function of the Hg/Te flux ratio. At both the lowest and highest Hg/Te ratios (183 and 550), hillock densities are very high, 1.3×10^{6} and 2.9×10^{5} cm^{-2}, respectively. The best surface morphology with our lowest hillock density of 1.5×10^{4} cm^{-2} was obtained with a HgTe flux ratio of 280. Of particular significance is that the hillock density depends more dramatically on the Hg pressure at lower values of the Hg/Te flux ratio compared to higher values as shown in Fig. 4.

The fact that all hillocks on one epilayer have nearly the same size indicates that they are generated during the first stage of epitaxially growth, where twins occur near or at the interface between the epilayer and substrate, and then propagate during growth to form pyramidal hillocks.[1] These twins can originate either from the substrate[2] or from the epilayer during the initial stage of epitaxially growth. If the growth parameters are not held constant during the entire growth period, then twins might possibly originate during later stages of epitaxially growth but hillock size wound not be uniform. According to the hillock model of Million *et al.*,[1] all hillocks should have the same orientation and size which is given by $\sqrt{2}d$, where d is the layer thickness. Their model is a good approximation of the results in this investigation, [see, for example, Figs. 3(a) and 3(b)]. It has been reported[4,5] that excess Hg pressure strongly influences twin formation, which explains the behavior of the hillock densities in the higher Hg flux region in Fig. 4. The mechanism of the hillock density dependence in the lower Hg flux region is not clear, but is possibly due to the occurrence of anti-phase twins caused by excess Te,[4] Te precipitates, or the effects of a rough surface caused by much lower Hg pressures. It is noteworthy to mention that this dependence of hillocks on Hg/Te flux ratio as shown in Fig. 4 is similar to a previously reported twin free growth dependence for the (111) *B* orientation.[3,28]

As discussed above, pyramidal hillocks are either related to the substrate surface or its preparation, or to the growth conditions. They can be reduced to a substrate limiting value by optimizing the growth conditions. Our best

result of 1.5×10^4 cm^{-2} was obtained with a Hg/Te flux ratio of 280 for the growth temperature of 180 °C.

C. The influence of the Hg/Te flux ratio on electrical properties

In order to understand the effects of Hg pressure on electrical properties, and to determine if electrical properties are correlated with structural defects, transport measurements were carried out on a series of samples with x values of 0.206 ± 0.005. Three samples with a slightly smaller x value are included in the hillock density dependence on the Hg/Te flux ratio but not in the dependence of electrical properties. All the samples under consideration were n-type. The electron concentration, as determined by the van der Pauw method, is in good agreement with the value obtained using the standard Hall geometry. The electron concentration was also calculated from the SdH oscillations assuming a spherical Fermi surface. The resulting electron concentrations are larger than the Hall effect results by a factor of 1.6–10, even though the assumptions involved should result in a discrepancy of at most a factor of 2. The SdH oscillations were shown to be three-dimensional and hence not due to an interface effect. Furthermore, reducing the thickness of the Hall geometry of one of the samples by etching with a solution of Br in ethylene glyocol, resulted in no measurable change in the electron concentration as determined both by means of the Hall effect and the SdH oscillations. Therefore, in spite of the discrepancy in the electron concentration, which is not yet understood, both the Hall effect and the SdH oscillations appear to result from the same three-dimensional electrons in the epilayer. Hence the electron concentration as determined by means of the Hall effect will be used in the following unless otherwise stated. Similarly the Hall mobility will be employed, keeping in mind the rather large uncertainty in the electron concentration and the possible uncertainty in the electron mobility. The electron concentration at both 300 and 10 K is a function of the Hg/Te flux ratio as shown in Fig. 5. Here only epilayers with an x value of 0.206 ± 0.005 are included. At room temperature the concentration is nearly independent of the Hg/Te flux ratio with the exception of an appreciable increase in concentration at Hg/Te flux ratios above approximately 450, where the $Hg_{1-x}Cd_xTe$ epilayers are degenerate. The behavior of the electron concentration at 10 K is similar except the values scatter more than an order of magnitude for values of the Hg/Te flux ratio between 250 and 420. The concentration as calculated from the SdH oscillations for 5 of these samples seem to scatter less, as can be seen in Fig. 5.

Figure 6 shows three typical examples of electron concentration versus reciprocal temperature. One curve corresponds to the sample grown with the Hg/Te ratio of 280 which is the optimum value as far as pyramidal hillocks are concerned. As can be seen in Fig. 6, the electron concentration decreases as the temperature is lowered, showing typical freeze out behavior. The other two curves are the results for the samples grown at the highest and the lowest limits of the Hg/Te flux ratio, namely 550 and 183, respectively. The electron concentration is very high for the largest value of the Hg/Te flux ratio. In $Hg_{1-x}Cd_xTe$ epilayers, nonstoichiometry is usually the result of Hg vacancies and interstitials. Excess Hg could be incorporated as an interstitial and act as a doubly ionized donor according to Stevenson and Tang.[29] Our results, which show a rapid increase in electron concentration with an increasing Hg/Te ratio above a value of 400, agree well with the above statement. On the other hand, the electron concentration seems to increase when the Hg/Te flux is decreased below a value of 250, although this increase is not as fast compared to the high Hg/Te flux region. Because of the

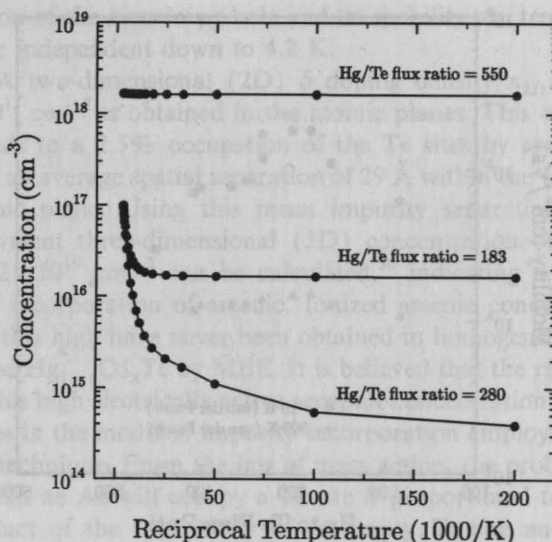

FIG. 5. Typical examples of electron concentrations vs reciprocal temperature.

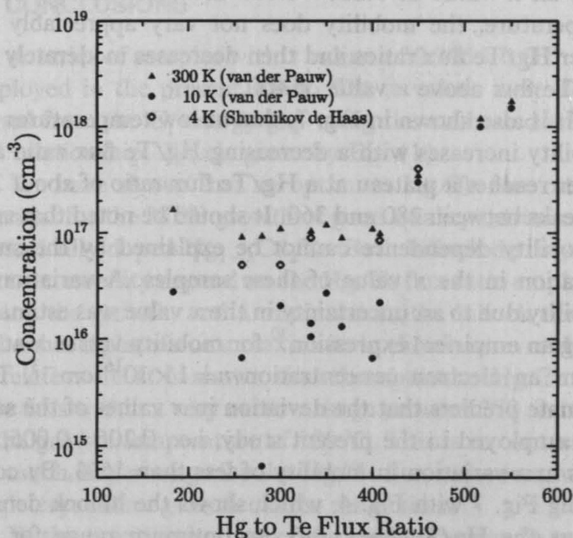

FIG. 6. Electron concentration vs Hg/Te flux ratio for the $Hg_{1-x}Cd_xTe$ epilayers with an x value of 0.206 ± 0.005. The Hall effect results at 300 and 10 K are shown as filled triangles and circles, respectively. The electron concentration as calculated from SdH oscillations at 4.2 K are displayed as empty circles.

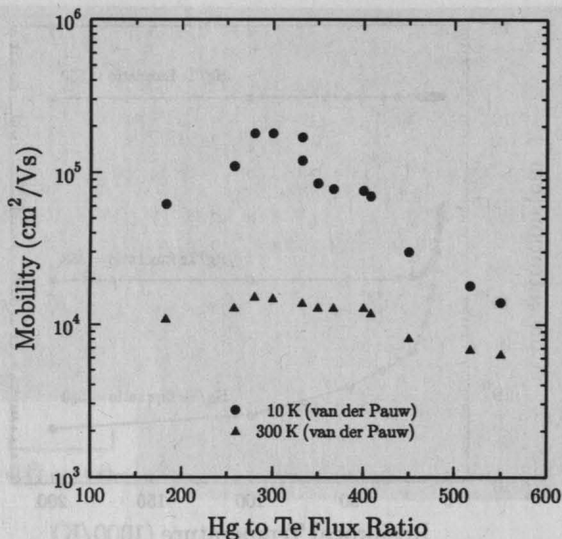

FIG. 7. Electron mobility vs the Hg/Te flux ratio for the $Hg_{1-x}Cd_xTe$ epilayers with an x value of 0.206±0.005. The mobilities at 300 and 10 K are shown as filled triangles and circles, respectively.

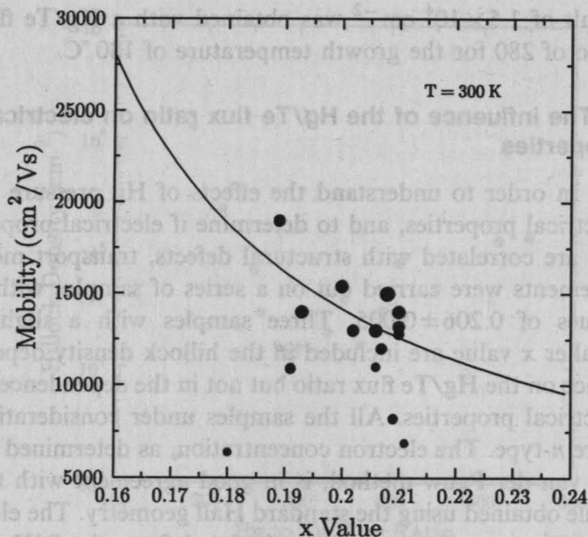

FIG. 8. The electron mobility at 300 K of all samples investigated vs their x value. Here the curve is an empirical relationship for undoped bulk $Hg_{1-x}Cd_xTe$ according to Higgins *et al.* (see Ref. 31). The larger circles fall close to this curve. The size of the circles is an indication of the Hg/Te flux ratio, i.e., the larger the circle the closer the Hg/Te flux ratio is to the optimum value of 300.

presence of only one sample with a Hg/Te flux ratio below 250 and the large scatter in the concentration data mentioned above, this last observation may not be generally correct. A possible explanation for a Hg/Te flux ratio dependence in this region is the presence of tellurium atoms at antisite positions, i.e., on Hg sites.[4,5] Alternatively, n-type impurities present in either the source material or in the substrates, which are incorporated in the metal sublattice, may be responsible for higher concentrations in the lower Hg pressure region.[6]

The electron mobility as determined from the Hall effect results at both 300 and 10 K, is a function of the Hg/Te flux ratio as shown in Fig. 7, where only epilayers with an x value of 0.206±0.005 are included. At room temperature, the mobility does not vary appreciably for lower Hg/Te flux ratios and then decreases moderately for Hg/Te flux above a value of 400.

It is also shown in Fig. 7, that at low temperatures the mobility increases with a decreasing Hg/Te flux ratio and either reaches a plateau at a Hg/Te flux ratio of about 360 or peaks between 280 and 360. It should be noted that such a mobility dependence cannot be explained by the small deviation in the x value of these samples. A variation in mobility due to an uncertainty in the x value was estimated using an empirical expression[30] for mobility versus x at 4.5 K for an electron concentration $n=1\times10^{16}$ cm^{-3}. This estimate predicts that the deviation in x values of the samples employed in the present study, i.e., 0.206±0.005, results in a variation in mobility of less than 15%. By comparing Fig. 7 with Fig. 4, which shows the hillock density versus the Hg/Te flux ratio, an optimum range for the Hg/Te flux ratio between 280 and 360 is apparent, i.e., the hillock density displays a minimum between 280 and 360, and the mobility has either a plateau at a Hg/Te flux ratio above approximately 360 or peaks at a Hg/Te flux ratio between 280 and 360.

The mobility of all the samples investigated at 300 K is plotted versus their x value in Fig. 8. Here the curve is an empirical relationship for undoped bulk $Hg_{1-x}Cd_xTe$ according to Higgins *et al.*[31] The larger circles fall close to this curve, where the size of the circle is an indication of the Hg/Te flux ratio; the larger the circle the closer the Hg/Te flux ratio is to the optimum value of 300.

At low temperatures ionized impurity scattering is the dominant factor for the electron mobility of narrow gap $Hg_{1-x}Cd_xTe$.[32,33] The scattering centers are either foreign extrinsic impurities or electrically active structural defects such as twins and nonstoichiometric defects consisting of Hg interstitials and vacancies or Te antisites. Because all the samples in Fig. 7 were grown in the same environment with the exception of the Hg flux, the influence of foreign impurities can reasonably be considered to be the same. As mentioned above, a minimum in the hillock density coincides with larger mobilities. It is obvious that optimizing the Hg/Te flux ratio is very important; this improves the structural quality, i.e., reduces the hillock density and the number of defects due to nonstoichiometry, which should improve the electrical properties.

D. Atomic sheet doping with As

In order to enhance the substitional incorporation of As, and to establish a new alternative to narrow gap $Hg_{1-x}Cd_xTe$ doping techniques, experiments were carried out using the suspension of growth in order to incorporate atomic planes of As. This technique, atomic sheet doping, was originally proposed by Wood *et al.*[34] to improve the doping profile in MBE grown GaAs and has become an important technology in advanced III-V semiconductor device concepts.[35]

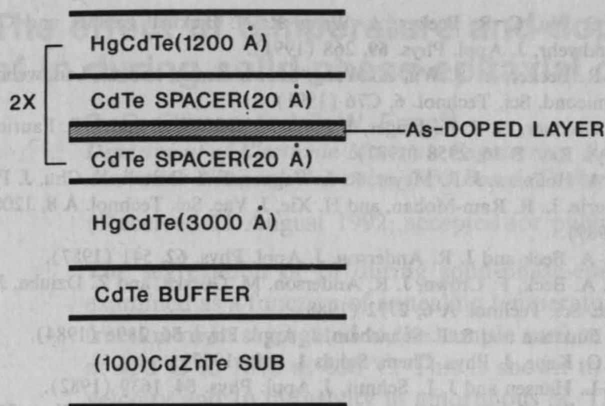

FIG. 9. Schematic diagram of the δ doped sample structure.

The sample structure, as shown in Fig. 9, consists of two single As-doped atomic planes. The 20 Å spacer layers, which are actually composed of $Hg_{0.3}Cd_{0.7}Te$, provide holes for the narrow gap $Hg_{0.77}Cd_{0.23}Te$. The carrier concentration and Hall mobility versus temperature is shown in Fig. 10. The Hall coefficient changes sign at about 110 K. At 70 K, the hole concentration is approximately 5×10^{17} cm^{-3} and the hole mobility is about 180 cm^2/V s. Both are almost independent of temperature below 70 K. No evidence of freeze out at low temperatures is observed in Fig. 10, because of the spatial separation of the parent impurity ions and the holes. The results were further confirmed by a more detailed study using a multicarrier mobility spectrum analysis.[16,17] This analysis showed that at 220 K, there is mixed conduction involving electrons and two kinds of holes. Below approximately 120 K, the electron conductivity disappears, the light hole conductivity can no longer be resolved by this method, and the concentration of the remaining hole and its mobility are temperature independent down to 4.2 K.

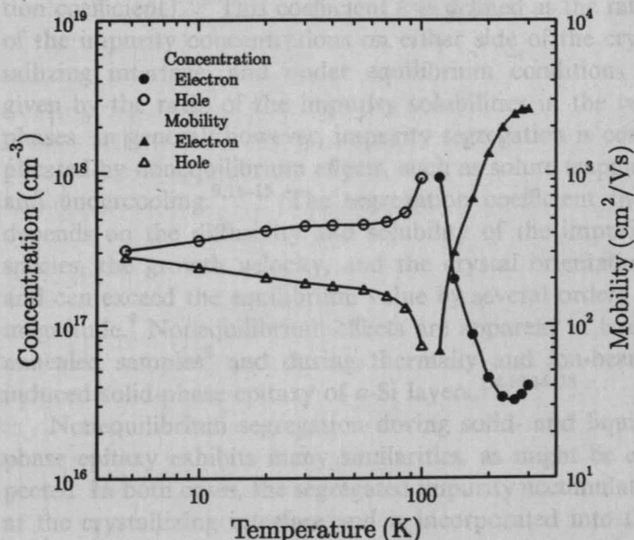

FIG. 10. Van der Pauw charge carrier concentration and mobility vs temperature for the δ doped sample.

A two-dimensional (2D) δ doping density $n_{2D}=1.2\times10^{13}$ cm^{-2} is obtained in the atomic planes. This corresponds to a 2.5% occupation of the Te sites by arsenic, with an average spatial separation of 29 Å within the (100) atomic plane. Using this mean impurity separation, an equivalent three-dimensional (3D) concentration of $n_{3D}=4.2\times10^{19}$ cm^{-3} can be calculated,[36] indicating a very high incorporation of arsenic. Ionized arsenic concentration this high have never been obtained in homogeneously doped $Hg_{1-x}Cd_xTe$ by MBE. It is believed that the reason for this high electrically active acceptor concentration originates in the modified impurity incorporation employed in this technique. From the law of mass action, the probability that an As will occupy a Te site is proportional to the product of the availability of an empty Te site and an exponential term containing an activation energy. In the δ doping process, As atoms are evaporated onto the static surface during a growth interruption after a cation-stabilized surface had been established by opening the Cd shutter. The RHEED patterns exhibit a mixture of a strong $c(2\times2)$ and a faint (2×1) reconstruction. Therefore the availability of unoccupied metal sites for As atoms which impinge on the surface is much reduced when compared to the availability of unoccupied metal sites in other doping processes. The present results corraborate the working hypothesis that establishing a cation-stabilized surface is a key point in substitional incorporation of As.[10] In fact, we have recently shown that laser illumination has a similar effect on the surface by increasing the desorption of Te during CdTe growth.[12] The present successes in obtaining highly doped p-type $Hg_{1-x}Cd_xTe$ using the atomic-sheet doping technique provides a new alternative method to obtain p-type $Hg_{1-x}Cd_xTe$.

IV. CONCLUSIONS

A series of samples with x values of 0.206 ± 0.005 were employed in the present study. The x values were determined from the E_1 energy gap using the calibrated empirical relationship, $E_1(x)$, given by Eq. (1).

We have shown that an optimum Hg/Te flux ratio is essential for the MBE growth of good quality intrinsic and extrinsically doped $Hg_{1-x}Cd_xTe$. Both hillock density and electron mobility depend on the Hg/Te flux ratio employed during the growth, and a minimum in the hillock density and either a plateau or a maximum in the electron mobility correlate well. It is shown that the optimum Hg/Te flux ratio falls within a very narrow range between 270 and 360, at the growth temperature of 180 °C. This is in contrast to the much larger range for the Hg/Te flux ratio over which single crystalline growth can be maintained.

With an understanding of the necessary growth conditions for good intrinsic material, extrinsic doping of As using the δ doping technique has been demonstrated and a very high atomic sheet density is obtained. The results are encouraging and it is expected that the present success in As doping is an important step in understanding the dop-

ing mechanism and in developing new methods for device fabrication using Hg based materials.

ACKNOWLEDGMENTS

This work was supported by the Bundesministerium für Forschung and Technologie and the Alexander von Humboldt Stiftung. In addition the authors wish to thank A. Schönteich for maintaining and making the necessary changes in the MBE system. Furthermore the AEG company in Heilbronn, Germany provided excellent CdTe source material which improved the electrical properties of our $Hg_{1-x}Cd_xTe$.

[1] A. Million, L. DiCicio, J. P. Gailliard, and J. Piaguet, J. Vac. Sci. Technol. A 6, 2813 (1988).
[2] R. J. Koestner and H. F. Schaake, J. Vac. Sci. Technol. A 6, 2834 (1988).
[3] K. A. Harris, T. H. Myers, R. W. Yanka, K. A. Harris, L. M. Mohnkern, R. W. Green, and N. Otsuka, J. Vac. Sci. Technol. A 8, 1013 (1990).
[4] J. P. Faurie, R. Sporken, S. Sivananthan, and M. D. Lange, J. Cryst. Growth 111, 698 (1991).
[5] R. J. Koestner, M. W. Goodwin, and H. F. Schaake, J. Vac. Sci. Technol. B 9, 1731 (1991).
[6] M. Boukerche, P. S. Wijewarnasuriya, S. Sivananthan, I. K. Sou, Y. J. Kim, K. K. Mahavadi, and J. P. Faurie, J. Vac. Sci. Technol. A 6, 2830 (1988).
[7] C. J. Summers, R. G. Benz II, B. K. Wagner, J. D. Benson, and D. Rajavel, Proc. SPIE 1, 1106 (1989).
[8] J. W. Han, S. Hwang, Y. Lansari, R. L. Harper, Z. Yang, N. C. Giles, J. W. Cook, Jr., J. F. Schetzina, and S. Sen, J. Vac. Sci. Technol. A 7, 305 (1989).
[9] R. N. Bicknell, N. C. Giles, and J. F. Schetzina, Appl. Phys. Lett. 49, 1095 (1986).
[10] J. M. Arias, S. H. Shin, D. E. Cooper, M. Zandian, J. G. Pasko, E. R. Gertner, and J. Singh, J. Vac. Sci. Technol. A 8, 1025 (1990).
[11] J. Benson, D. Rajavel, B. Wagner, R. Benz II, and C. J. Summers, J. Cryst. Growth 95, 543 (1989).
[12] Y. S. Wu, C. R. Becker, A. Waag, R. N. Bicknell-Tassius, and G. Landwehr, J. Appl. Phys. 69, 268 (1991).
[13] C. R. Becker, Y. S. Wu, A. Waag, M. M. Kraus, and G. Landwehr, Semicond. Sci. Technol. 6, C76 (1991).
[14] Y. Guldner, G. S. Boebinger, J. P. Vieren, M. Voos, and J. P. Faurie, Phys. Rev. B 36, 2958 (1987).
[15] C. A. Hoffman, J. R. Meyer, R. J. Wagner, F. J. Bartoli, X. Chu, J. P. Faurie, L. R. Ram-Mohan, and H. Xie, J. Vac. Sci. Technol. A 8, 1200 (1989).
[16] W. A. Beck and J. R. Anderson, J. Appl. Phys. 62, 541 (1987).
[17] W. A. Beck, F. Crown, J. R. Anderson, M. Gorska, and Z. Dziuba, J. Vac. Sci. Technol. A 6, 2772 (1988).
[18] E. Finkman and S. E. Schacham, J. Appl. Phys. 56, 2896 (1984).
[19] E. O. Kane, J. Phys. Chem. Solids 1, 249 (1957).
[20] G. L. Hansen and J. L. Schmit, J. Appl. Phys. 54, 1639 (1982).
[21] G. L. Hansen, J. L. Schmit, and T. N. Casselman, J. Appl. Phys. 53, 7099 (1982).
[22] S. Katsuki and M. Kunimune, J. Phys. Soc. Jpn. 31, 415 (1971).
[23] R. Ludeke and W. Paul, J. Appl. Phys. 37, 3499 (1966).
[24] R. R. Galazka and A. Kisiel, Phys. Status Solidi 34, 63 (1969).
[25] A. Moritani, K. Taniguchi, C. Hamaguchi, and J. Nakai, J. Phys. Soc. Jpn. 36, 79 (1973).
[26] A. Kisiel, M. Podgorny, A. Rodzik, and W. Giriat, Phys. Status Solidi B 71, 457 (1975).
[27] E. Finkman and Y. Nemirovsky, J. Appl. Phys. 50, 4356 (1979).
[28] R. W. Yanka, K. A. Harris, L. M. Mohnkern, and T. H. Myers, J. Cryst. Growth 111, 715 (1991).
[29] D. A. Stevenson and M-F. S. Tang, J. Vac. Sci. Technol. B 9, 1615 (1991).
[30] P. M. Raccah, J. W. Garland, Z. Zhang, A. H. M. Chu, J. Reno, I. K. Sou, M. Boukerche, and J. P. Faurie, J. Vac. Sci. Technol. A 4, 2077 (1986).
[31] W. M. Higgins, G. N. Pultz, R. G. Roy, and R. A. Lancaster, J. Vac. Sci. Technol. A 7, 271 (1989).
[32] D. Long, Phys. Rev. 176, 923 (1968).
[33] W. Scott, J. Appl. Phys. 43, 1055 (1972).
[34] C. E. C. Wood, G. Metze, J. Berry, and L. F. Eastman, J. Appl. Phys. 51, 383 (1979).
[35] K. Ploog, M. Hauser, and A. Fischer, Appl. Phys. A 45, 233 (1988).
[36] E. F. Schubert, J. E. Cunningham, and W. T. Tsang, Solid State Commun. 63, 591 (1987).